frontiers | Frontiers in Materials

ORIGINAL RESEARCH
published: 07 April 2022
doi: 10.3389/fmats.2022.859342

Diffraction-based Residual Stress Mapping of a Stress Frame of Gray Iron via Vibratory Stress Relief Method

Shi-Wei Chen[1], E-Wen Huang[2]*, Sung-Mao Chiu[3], Mark Reid[4], Cheng-Yen Wu[3], Anna M. Paradowska[4,5], Tu-Ngoc Lam[2,6]*, Yu-Hao Wu[2], Soo Yeol Lee[7], Shao-Chien Lu[8], Shin-An Chen[9], Yan-Gu Lin[1] and Shih-Chang Weng[1]*

[1]National Synchrotron Radiation Research Center, Hsinchu, Taiwan, [2]Department of Materials Science and Engineering, National Yang Ming Chiao Tung University, Hsinchu, Taiwan, [3]Metal Industries Research and Development Centre, Kaohsiung, Taiwan, [4]Australian Nuclear Science and Technology Organisation (ANSTO), Lucas Heights, NSW, Australia, [5]School of Civil Engineering, The University of Sydney, Sydney, NSW, Australia, [6]Department of Physics, College of Education, Can Tho University, Can Tho, Vietnam, [7]Department of Materials Science and Engineering, Chungnam National University, Daejeon, South Korea, [8]Department of Mechanical Engineering, National Yang Ming Chiao Tung University, Hsinchu, Taiwan, [9]Department of Engineering and System Science, National Tsing Hua University, Hsinchu, Taiwan

OPEN ACCESS

Edited by:
Dongchan Jang,
Korea Advanced Institute of Science and Technology, South Korea

Reviewed by:
Pavlo Maruschak,
Ternopil Ivan Pului National Technical University, Ukraine
Jianan Hu,
Independent researcher, Guildford, United Kingdom

***Correspondence:**
Shi-Wei Chen
chen.sw@nsrrc.org.tw
E-Wen Huang
ewenhuang@nctu.edu.tw
Tu-Ngoc Lam
lamtungoc1310@nctu.edu.tw

Specialty section:
This article was submitted to Mechanics of Materials, a section of the journal Frontiers in Materials

Received: 21 January 2022
Accepted: 07 March 2022
Published: 07 April 2022

Citation:
Chen S-W, Huang E-W, Chiu S-M, Reid M, Wu C-Y, Paradowska AM, Lam T-N, Wu Y-H, Lee SY, Lu S-C, Chen S-A, Lin Y-G and Weng S-C (2022) Diffraction-based Residual Stress Mapping of a Stress Frame of Gray Iron via Vibratory Stress Relief Method. Front. Mater. 9:859342. doi: 10.3389/fmats.2022.859342

The role of residual stress is critical, particularly for machine tools demanding accuracy below 1 μm. Although minor stresses are subjected to a tiny area, the applied force can cause devastating distortions on the precision components at this length scale. In this research, we systematically investigated the residual stress in a stress frame of the gray iron used in machine tools using synchrotron X-ray and neutron sources. Through the combination of these techniques, the residual stresses on the surface, inside the bulk, and in average were presented. Comprehensive analysis results shed light on the vibratory stress relief technique, which reduced the residual stresses and stabilized them, even materials undergoing cycling heating. Although compressive stresses are not effectively reduced, this technique is useful in improving the mechanical stability of the materials in machine tools.

Keywords: gray iron, residual stress, synchrotron X-ray, neutron diffraction, machine tools + design

INTRODUCTION

Machine tools including cutting machines and drilling machines are used to manufacture products with specific shapes and dimensional tolerances. The work presented here is not only fundamental in nature but also important to the machine tool industry. The demand of machine tools increases year by year due to technology developments and the associated increased requirements for machining accuracy. According to Mou and Liu, (1992); Mou, (1997); Anderson, (2012), accuracy requirements are routinely 1 μm or less and cyclic stability is also required for high-precision machine tools. To do that, the material components of the machine tools must be stable during operation. Any issues disturbing the stability of the components during casting or machining should be avoided. One such issue is the residual stress existing in the components of machine tools, arising from the manufacturing process. Any release of the residual stress or the interaction between the components may cause a decreased strength or distortion, resulting in reduced accuracy of the

machine tools. Controlling the residual stress, thus, becomes crucial to develop high-precision machine tools with both high accuracy and stability during operation.

A number of methods are available for measuring the residual stress, including hole drilling methods reported by Gliha et al., (2013); Huang et al., (2013), contour methods and ultrasonic methods presented by Sanderson and Shen, (2010); Xu et al., (2015), and diffraction techniques utilizing X-ray or neutrons shown by Huang et al., (2011); Lee et al., (2015); Brown et al., (2016); Lee et al., (2017); Seo et al., (2017); Lam et al., (2020). Hole drilling and contour methods as destructive techniques are not well-accepted in the industry. Ultrasonic methods measure the residual stress based on the variation of sound speed after passing through or along the sample. However, the microstructure of the samples will also contribute to variation in ultrasound speed, and it is not easy to distinguish the effect of residual stress and that of microstructure. X-ray diffraction techniques are widely used because they are nondestructive methods and available as portable units, greatly speeding up the generation of results and its application in the industry. However, the resolution of the instrument is often neglected, and thus the value of the measured residual stress is potentially unreliable. In the X-ray diffraction method, resolution is dominated by the energy resolution of the X-ray and angular resolution of the diffractometer, according to Bragg's Law. The combined energy resolution of the X-ray source and angular resolution of the diffractometer should be kept below 10^{-4} to determine the residual stress in steels and alloys as the order of the residual strains may be below 10^{-4}. With sufficient resolution, peak shifts arising due to the residual strain can be identified correctly, and thus reasonable values of the residual stress can be obtained.

In-house X-ray diffraction instruments or portable X-ray diffraction instruments with X-ray tubes of the beam size are controlled by slits. The X-ray beam is generally not focused effectively in reducing the flux available for the measurement. A large X-ray beam size, while increasing flux, will result in the diffracted peak being broadened and hinder the identification of peak shift. In addition, the X-ray beam is dispersive as it is emitted from the X-ray tube, which complicates Bragg's diffraction. The most critical factor of in-house X-ray machines is the energy resolution, which may be insufficient to identify the residual strain/stress precisely. As presented by Ricardo A. Terini et al., (1999), characteristic X-ray spectra emitted from a Philips MCN 421 shows an energy resolution larger than 0.01 keV, which is too large for the residual stress measurement.

Synchrotron X-ray with both high flux and high-energy resolution is a very good source for collecting diffraction patterns, determining peak shifts, and identifying the residual strain in the materials. In this study, we used synchrotron X-ray and a 6-circle diffractometer to collect the diffraction patterns and estimate the residual strain in gray iron, an important property of machine tools. The synchrotron beamline is equipped with a horizontal mirror, vertical mirror, and double crystal monochromator (DCM) to focus the X-ray beam and precisely control the X-ray energy. The energy resolution of synchrotron X-ray is of the order of 10^{-4} eV. The 6-circle diffractometer with an angular resolution better than 0.003° is used to facilitate sample positioning. Both the X-ray energy resolution and accurate positioning of the samples allow us to obtain reliable values of the residual strain and subsequently stress. The method is successfully used to identify the residual stress in gray iron after vibratory stress relief treatment and cyclic heat treatment. As the penetration of X-ray in the iron-based materials is limited due to the high attenuation of X-ray by iron, the diffraction measurements only provide information on the residual stress state of the sample surface. In addition, we utilized a neutron source and diffraction method to determine the residual strains and subsequently stresses in the gray iron samples. High penetration of neutrons through iron-based materials allows the measurement of bulk stresses within the samples. Both average stresses in the bulk and stresses in the through-thickness of the samples are reported here. The results shown in this study, thus, can be the fundamentals of measuring the residual stress precisely and controlling the stability of components in the machine tools.

The vibratory stress relief technique has been shown to be an effective method for reducing the residual stress in metallic materials; however, the mechanism of stress relief is poorly understood. Comprehensive analyses of the stresses on the surface and inside the bulk of the gray iron samples obtained in this study will provide a new insight into the mechanism of vibratory stress relief.

MATERIALS AND METHODS

Materials

A gray iron, JIS FC 300, was fabricated by casting in a stress frame mold with a size of 200 mm, 100 mm, and 20 mm (length, width, and thickness, respectively), as shown in **Figure 1**. The stress frame has two thin rods outside and one thick rod inside to produce compressive stress and tensile stress after casting, respectively, due to different shrinkage suggested by Gustafsson et al., (2009); Pal, (2017). The material after casting was treated with annealing and vibratory stress relief treatment referring to Dawson and moffat, (1980); Wang et al., (2013); Wang et al., (2014); Wang et al., (2015). The samples in each condition (as cast, annealed, and annealed and vibratory stress relief) were subsequently subjected to cyclic heating. The vibratory stress relief treatment was conducted with a modified motor and adapter to vibrate the material at a frequency of 80–120 Hz. The load current of the stress relief motor was controlled to reach an amplitude about ±15 m/s^2 gravity acceleration measured by an amplitude sensor. The cyclic heat treatment was applied by heating and cooling from 28 to 90°C for 20 cycles. In this study, the investigated as-cast gray iron comprised presumably large grain sizes with relatively uniform distribution; thus, the effect of the microdefects originating from the heterogenous grain sizes (Wang et al., 2018) can be neglected.

X-Ray Diffraction Measurement

Synchrotron X-ray measurements were conducted at the BL07 beamline in the National Synchrotron Radiation Research Center (NSRRC), Taiwan. Before measurement, the beamline was

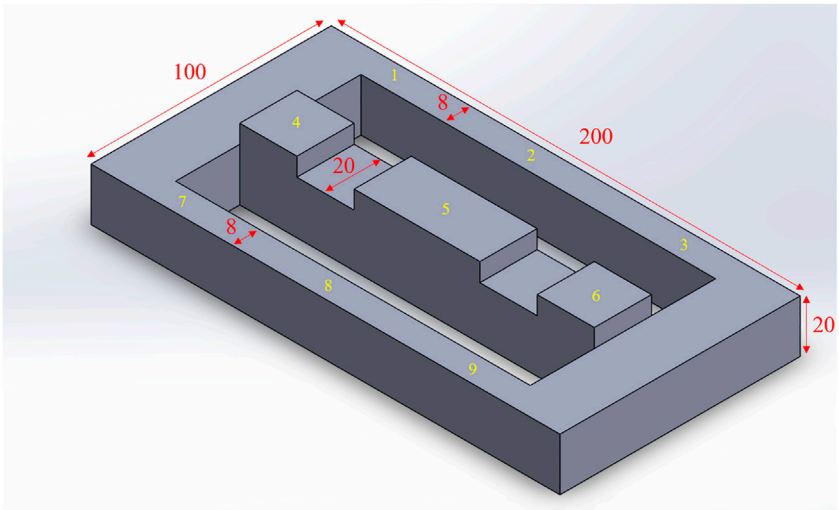

FIGURE 1 | Picture of the stress frame (unit: mm). L (longitudinal), N (through-thickness), and T (transverse) stand for the three orthogonal directions in the stress frame.

optimized by adjusting the vertical focus mirror, horizontal focus mirror, K-B mirror, and Si (111) double crystal monochromator (DCM) to obtain maximum intensity and the smallest divergence of the X-ray beam. The energy resolution of synchrotron X-ray was 10^{-4} eV at an energy of 18 KeV. The penetration depth was estimated to be 70 μm.

X-ray diffraction patterns were recorded at the BL07 beamline by utilizing a 6-circle diffractometer manufactured by Bruker. The incident and diffracted angles were fixed to collect the α-ferrite (BCC) diffraction peak of (211). Peak position, peak intensity, and peak width were obtained by a single-peak fitting procedure using a pseudo-Voigt function. The lattice strain (elastic strain) was calculated as follows:

$$\varepsilon_{hkl} = \frac{d_{hkl} - d_{0,hkl}}{d_{0,hkl}} \tag{1}$$

where $d_{0,hkl}$ is the stress-free d-spacing.

Plane Stress Condition

Because of the low penetration of X-ray in gray iron, it was assumed that the residual stress was in a plane stress condition. The azimuthal-dependent lattice strains can be expressed as follows:

$$f_{xx}\varepsilon_{xx} + f_{xy}\varepsilon_{xy} + f_{yy}\varepsilon_{yy} + f_{xz}\varepsilon_{xz} + f_{yz}\varepsilon_{yz} = \varepsilon_{hkl}^{\Phi} \tag{2}$$

where ε_{ij} is the strain tensor component and f_{ij} is a function of diffraction geometry.

Details of the theory can be found in the references reported by He, (2000); He, (2009). Based on the experimental geometry in this study, a plane stress condition was assumed as the external load to the thin plate sample, where $\sigma_{zz} = \sigma_{xz} = \sigma_{yz} = 0$, $\varepsilon_{xz} = \varepsilon_{yz} = 0$. The equation can be further reduced to

$$f_{xx}\varepsilon_{hkl,xx} + f_{xy}\varepsilon_{hkl,xy} + f_{yy}\varepsilon_{hkl,yy} = \varepsilon_{hkl}^{\Phi} \tag{3}$$

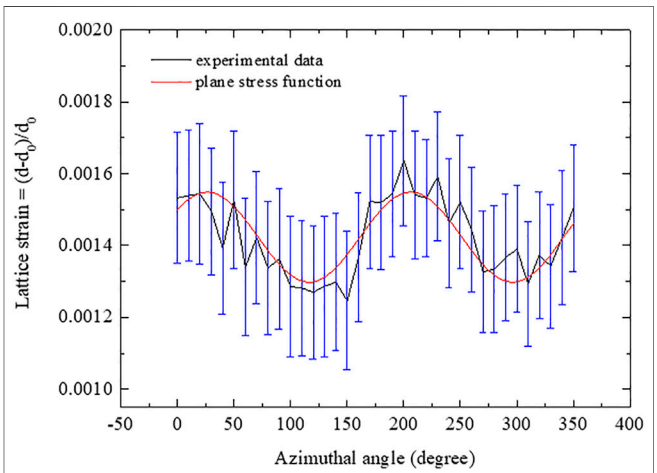

FIGURE 2 | Curves of the lattice strain varying with the azimuthal angle. The experimental curve (black line) and the curve calculated by the plane stress function (red line).

where,

$$f_{xx} = \sin^2\varphi\cos^2\theta \tag{4}$$

$$f_{xy} = -\sin 2\varphi\cos^2\theta \tag{5}$$

$$f_{yy} = \cos^2\varphi\cos^2\theta \tag{6}$$

$$f_{yz} = -\cos\varphi\sin 2\theta \tag{7}$$

$$f_{zz} = \sin^2\theta \tag{8}$$

where θ is the peak position at the azimuthal angle φ. In the plane stress condition, the contribution of terms f_{yz} and f_{zz} can be neglected due to the small diffraction angle 2θ. Consequently, the equation was dominated by the first three terms, $\varepsilon_{hkl,xx}$, $\varepsilon_{hkl,xy}$, and $\varepsilon_{hkl,yy}$. By performing the linear least-squares regression of all the

measured azimuthal-dependent lattice strains, the normal and shear strain components ($\varepsilon_{hkl,xx}$, $\varepsilon_{hkl,yy}$, and $\varepsilon_{hkl,xy}$) of the material at the measured positions can be obtained as done by Wu et al., (2016). The azimuthal angle was controlled by rotating the sample with a high precise motor. **Figure 2** shows an example of the fitting.

Neutron Diffraction Measurement

The residual stress analyses of the gray iron samples using neutron diffraction were carried out at the TG3 beamline using the KOWARI residual strain instrument at the Australian Nuclear Science and Technology Organization (ANSTO), Australia. Due to the long penetration depth of neutrons, the KOWARI instrument can measure the residual stresses within the bulk of the material. By using an appropriate slit size, 3 × 3 mm slits on the primary beam and 3-mm radial collimators on the detector, spatially resolved measurements can be made within the samples. The results can subsequently be averaged to obtain a more generalized picture. The stresses are determined with the equation:

$$\sigma_x = \frac{E_x}{(1+v)(1-2v)}\Big((1-v)\varepsilon_x + v\big(\varepsilon_y + \varepsilon_z\big)\Big) \tag{9}$$

where the strains are calculated *via* **Eq. 1**, E and v are Young's modulus and Poisson's ratio, respectively.

Initially, the KOWARI instrument was optimized to maximize the neutron flux of the sample at a wavelength of 1.67 Å and to yield an approximately 90° diffraction angle for the α-ferrite diffraction peak of (211) and hence a cuboid gage volume. For a particular crystallographic direction being probed, Young's modulus and Poisson's ratio values were calculated using IsoDec software (Kröner model) proposed by Gnäupel-Herold, (2012). The sample was then translated and rotated on a sample stage to map out the strains in the three orthogonal directions.

Determination of Stress-Free D-Spacing

The stress-free d-spacing, $d_{0,hkl}$, strongly influences the determination of the residual stress. Even a tiny deviation of $d_{0,hkl}$ will cause a serious variation of the lattice strain. According to Withers et al., (2007), there are several reference standards to determine the stress-free d-spacing, including powders, filings, cubes, and combs. The main aim of all these methods is to utilize the free surface, as much as possible, as this is least likely to be constrained. This study probed the stress-free d-spacing by collecting the diffraction patterns from all the three directions at the corner of the samples as close as possible to the surface. The through-thickness direction (the thinnest) was then assumed to be in plain stress, and a $d_{0,hkl}$ was calculated *via* deconvolution. With this method, a reasonable stress-free d-spacing is achieved.

RESULTS AND DISCUSSION

Residual Stresses Measured by Synchrotron X-Ray

The residual stresses measured with synchrotron X-ray, assuming a plane stress condition, in the stress frame of the gray iron are shown in **Figure 3**. **Figure 3A** presents the residual stresses at point 2 (outside, thin), point 5 (middle, thick), and point 8 (outside, thin) of the stress frame before cyclic heating. As noted, the annealing process will enlarge the residual stresses and modify the stress distribution on the surface. One can expect this phenomenon, although annealing can facilitate the relaxation of the structure, and the material will experience additional thermal effects during cooling. Different cooling rates on the surface and inside the bulk will give rise to thermally induced residual stresses. Synchrotron X-ray measurement collected the diffraction patterns on the top surface of the sample. The thermal stress issue should be much more serious; thus, higher stress and confused distribution on the surface of the gray iron after annealing can be observed in **Figure 3A**. It can be realized that the vibratory stress relief technique can reduce the stress effectively. Not only ε_{xx} and ε_{yy}, shear stress ε_{xy} converged to zero when the material suffered from the vibratory stress relief treatment.

Figure 3B shows the residual stresses in the stress frame of the gray iron after cycling heating treatment, probed with synchrotron X-ray. Both the normal and shear stresses between casting, annealing, and annealing associated with the vibratory stress relief technique became unity after cycling heating, and there were no significant differences between them. It means that the cycling heating treatment can maintain and stabilize the residual stress on the surface of the material, even when the value of the stress was still high. The stabilized stress can help stabilize the size variation of the material. Because gray iron is an important material, being the components of machine tools, the stabilized stress and size variation will be very important for the machine tools to maintain high accuracy.

Residual Stresses Measured by Neutron Diffraction

Figure 4 shows the residual stress in the stress frame of the gray iron probed with a neutron diffraction technique. **Figures 4A,B** display the stresses of the material before and after cycling heating treatment, respectively. The value was obtained by averaging the stress in each depth. As noted in **Figure 4A**, only the stress component along L-direction manifested the variation of the residual stress at different points of the stress frame. The results meet one's expectation by using the stress frame which contains two thin plates outside and one thick plate in the middle. Due to different shrinkage as cooling, the outside plates display compressive stress, while the middle plate exhibits tensile stress. The interaction between compressive stress and tensile stress occurs along L-direction. The stress along L-direction of the stress frame was already evidenced by using a strain gage reported by Pal, (2017). The compressive stress state in the outside plates and tensile stress state in the middle plate of the stress frame were also observed in this study. As noted, points 1–3 and points 7–9 in the stress frame reveal the compressive stress, while points 4–6 present the tensile stress condition. Consistent results indicated that the measurement of the residual stress with a neutron source is reliable.

In **Figure 4A**, annealing and vibratory stress relief treatments can reduce the tensile stress at points 4–6, while the compressive

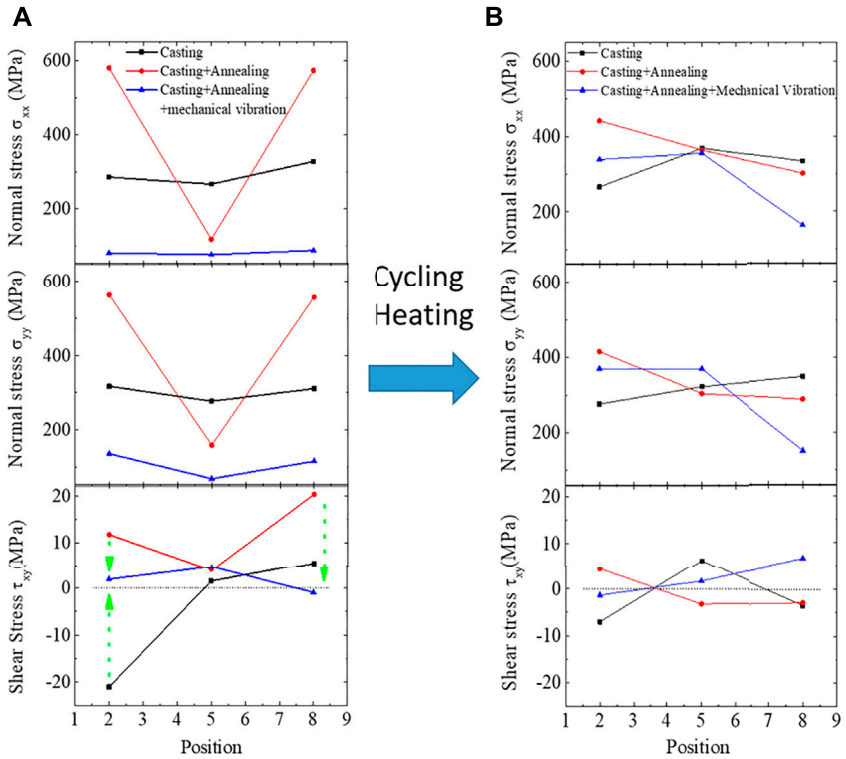

FIGURE 3 | Residual stresses at points 2, 5, and 8 of the stress frames **(A)** Initial stress, **(B)** Stress after cyclic heating.

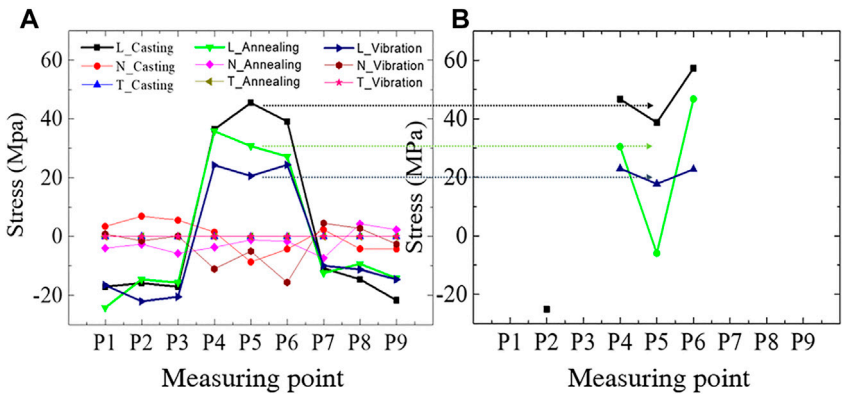

FIGURE 4 | Average stress in the stress frame of the gray iron along the three orthogonal directions probed with the neutron diffraction technique **(A)** before and **(B)** after cycling heating treatment.

stresses at points 1–3 and points 7–9 do not change evidently. The material with the tensile stress state is instable and the structure is loose. As a result, annealing and vibratory stress relief treatments can rearrange the atoms in the loose structure.

It is very interesting to compare the residual stresses in the gray iron after further cycling heating treatment. As indicated in **Figure 4B**, the residual stresses in the gray iron with the as-cast state and annealing state are altered violently after the cycling heating. The residual stress at points 4–6 becomes highly nonuniform after cycling heating. Only the gray iron with the vibratory stress relief treatment maintains almost the same value of the residual stress after cycling heating. It implies that the vibratory stress relief treatment can stabilize the residual state, even the materials experiencing further cyclic change in temperature.

The phenomenon was also revealed in the depth profile analysis of the residual stress in the gray iron after cycling in **Figure 5**. Gray iron with the vibratory stress relief treatment

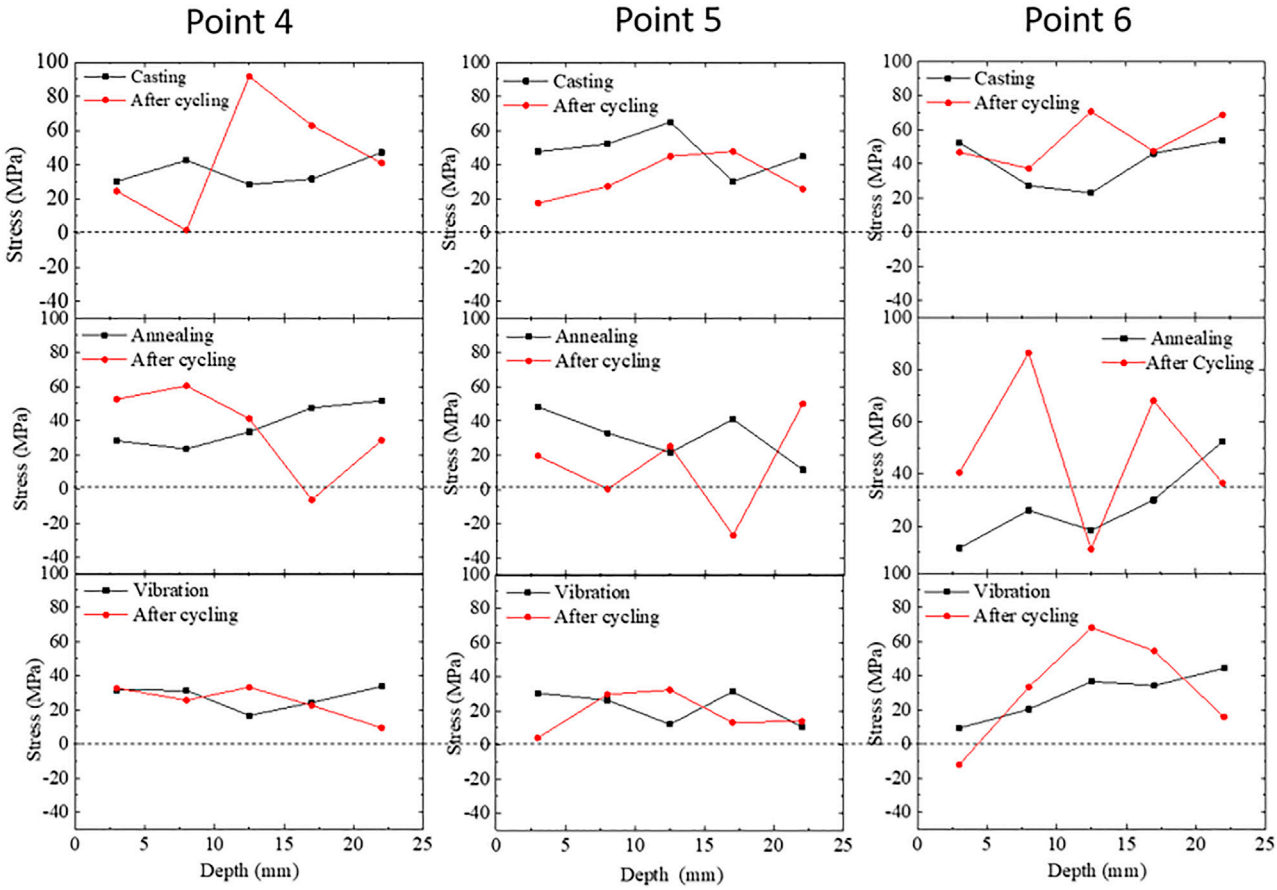

FIGURE 5 | Depth profile analysis of the residual stress in the stress frame of the gray iron with the three conditions after cycling heating.

shows similar residual stress distribution in depth, at point 5, after cycling heating, while the residual stresses in the other two states of materials vary irregularly with depth after cycling heating treatment. The results imply that the vibratory stress relief technique stabilizes the residual stress on the surface or inside the bulk of the gray iron, with the materials experiencing further cyclic heating treatment. It is interesting that the depth profile analysis does not disclose the specifically compressive stress on the surface of the material as usual. It is maybe due to the probing depth at the first point of 3 mm, which is not shallow enough to exhibit surface effect.

CONCLUSION

This study probed the residual stress in the gray casting iron with synchrotron X-ray and neutron sources. High-energy resolution of X-ray and neutron allows us to acquire reliable values of the stress. Such comprehensive measurements display the stress on the top surface, inside the bulk, and in average. The results indicated that the vibratory stress relief technique, rather than the annealing process, can effectively reduce the stress on the surface of the gray iron and stabilize the stress on the surface or inside the bulk, with the material experiencing further cycling heating treatment. The vibratory stress relief treatment can stabilize the size of the gray iron, a component of the machine tools. Therefore, the machine tools are characterized by high accuracy and stability.

DATA AVAILABILITY STATEMENT

The original contributions presented in the study are included in the article/Supplementary Material; further inquiries can be directed to the corresponding authors.

AUTHOR CONTRIBUTIONS

Conceptualization: S-WC, E-WH, and S-MC. Data analysis: S-WC, E-WH, S-MC, MR, and AP. Investigation: C-YW and S-CL. Design: S-MC and C-YW. Project administration: S-WC and E-WH. Resources: MR, AP, S-AC, Y-GL, and S-CW. Supervision: S-WC and E-WH. Writing—S-WC and E-WH. Writing—review and editing: T-NL, Y-HW, and SYL. All authors have read and agreed to the published version of the manuscript.

FUNDING

We thank the Ministry of Science and Technology (MOST) Programs of 108-2221-E-009-131-MY4 and MOST 110-2224-E-007-001. This work was financially supported by the "Center for the Semiconductor Technology Research" from the Featured Areas Research Center Program within the framework of the Higher Education Sprout Project by the Ministry of Education (MOE) in Taiwan. This work was supported by the Higher Education Sprout Project of the National Yang Ming Chiao Tung University and Ministry of Education (MOE), Taiwan. SYL was supported by a National Research Foundation (NRF) grant funded by the Korean government (2021R1A4A1031494, 2020R1I1A2070474).

ACKNOWLEDGMENTS

E-WH thanks the National Synchrotron Radiation Research Center (NSRRC) for Neutron Cultivation Program.

REFERENCES

Anderson, S. P. (2012). *Machine Tools: Design, Reliability and Safety*. UK: Nova Science Pub Inc.

Brown, D. W., Bernardin, J. D., Carpenter, J. S., Clausen, B., Spernjak, D., and Thompson, J. M. (2016). Neutron Diffraction Measurements of Residual Stress in Additively Manufactured Stainless Steel. *Mater. Sci. Eng. A* 678, 291–298. doi:10.1016/j.msea.2016.09.086

Dawson, R., and Moffat, D. G. (1980). Vibratory Stress Relief: A Fundamental Study of its Effectiveness. *J. Eng. Mater. Technol.* 102, 169–176. doi:10.1115/1.3224793

Gliha, V., Maruschak, P., and Vuherer, T. (2013). Behaviour of Short Cracks Emanating from Tiny Drilled Holes. *Mater. Tech.* 47, 441–446.

Gnäupel-Herold, T. (2012). ISODEC: Software for Calculating Diffraction Elastic Constants. *J. Appl. Crystallogr.* 45, 573–574.

Gustafsson, E., Hofwing, M., and Strömberg, N. (2009). Residual Stresses in a Stress Lattice-Experiments and Finite Element Simulations. *J. Mater. Process. Tech.* 209, 4320–4328. doi:10.1016/j.jmatprotec.2008.11.025

He, B. B. (2000). Stress Measurement with Two-Dimensional Diffraction. *P. Int. Cong. Experit. M.*, 943–945.

He, B. B. (2009). *Two-dimensional X-ray Diffraction*. New York: Wiley.

Huang, E.-W., Lee, S. Y., Woo, W., and Lee, K.-W. (2011). Three-Orthogonal-Direction Stress Mapping Around a Fatigue-Crack Tip Using Neutron Diffraction. *Metall. Mat Trans. A.* 43, 2785–2791. doi:10.1007/s11661-011-0904-8

Huang, X., Liu, Z., and Xie, H. (2013). Recent Progress in Residual Stress Measurement Techniques. *Acta Mechanica Solida Sinica* 26, 570–583. doi:10.1016/s0894-9166(14)60002-1

Lam, T.-N., Lee, S. Y., Tsou, N.-T., Chou, H.-S., Lai, B.-H., Chang, Y.-J., et al. (2020). Enhancement of Fatigue Resistance by Overload-Induced Deformation Twinning in a CoCrFeMnNi High-Entropy alloy. *Acta Materialia* 201, 412–424. doi:10.1016/j.actamat.2020.10.016

Lee, S.-Y., Ling, J., Wang, S., and Ramirez-Rico, J. (2017). Precision and Accuracy of Stress Measurement with a Portable X-ray Machine Using an Area Detector. *J. Appl. Cryst.* 50, 131–144. doi:10.1107/s1600576716018914

Lee, S. Y., Huang, E.-W., Woo, W., Yoon, C., Chae, H., and Yoon, S.-G. (2015). Dynamic Strain Evolution Around a Crack Tip under Steady- and Overloaded-Fatigue Conditions. *Metals* 5, 2109–2118. doi:10.3390/met5042109

Mou, J. (1997). A Systematic Approach to Enhance Machine Tool Accuracy for Precision Manufacturing. *Int. J. Machine Tools Manufacture* 37, 669–685. doi:10.1016/s0890-6955(95)00106-9

Mou, J., and Richard Liu, C. (1992). A Method for Enhancing the Accuracy of CNC Machine Tools for On-Machine Inspection. *J. Manufacturing Syst.* 11, 229–237. doi:10.1016/0278-6125(92)90023-9

Pal, A. M. J. (2017). Residual Stresses in Cast Iron Measurements and Simulations of Residual Stresses in Heat Treated Cast Iron Materials. Goeteborg: Department of Materials and Manufacturing Technology Chalmers University of Technology. Master's Thesis.

Sanderson, R. M., and Shen, Y. C. (2010). Measurement of Residual Stress Using Laser-Generated Ultrasound. *Int. J. Press. Vessels Piping* 87, 762–765. doi:10.1016/j.ijpvp.2010.10.001

Seo, S., Huang, E.-W., Woo, W., and Lee, S. Y. (2017). Neutron Diffraction Residual Stress Analysis during Fatigue Crack Growth Retardation of Stainless Steel. *Int. J. Fatigue* 104, 408–415. doi:10.1016/j.ijfatigue.2017.08.007

Terini, R. A., Costa, P. R., Furquim, T. A. C., and Herdade, S. B. (1999). Measurements of Discrete and Continuous X-ray Spectra with a Photodiode at Room Temperature. *Appl. Radiat. Isot.* 50, 343–354. doi:10.1016/s0969-8043(97)10123-3

Wang, J.-S., Hsieh, C.-C., Lai, H.-H., Kuo, C.-W., Wu, P. T.-Y., and Wu, W. (2015). The Relationships between Residual Stress Relaxation and Texture Development in AZ31 Mg Alloys via the Vibratory Stress Relief Technique. *Mater. Characterization* 99, 248–253. doi:10.1016/j.matchar.2014.09.019

Wang, J.-S., Hsieh, C.-C., Lin, C.-M., Chen, E.-C., Kuo, C.-W., and Wu, W. (2014). The Effect of Residual Stress Relaxation by the Vibratory Stress Relief Technique on the Textures of Grains in AA 6061 Aluminum alloy. *Mater. Sci. Eng. A* 605, 98–107. doi:10.1016/j.msea.2014.03.037

Wang, J. S., Hsieh, C. C., Liao, C. H., and Wu, W. (2013). The Effects of Waveform in Residual Stress Relief by Vibration Technique. *Trends Welding Res.*, 427–431.

Wang, Y. M., Voisin, T., Mckeown, J. T., Ye, J., Calta, N. P., Li, Z., et al. (2018). Additively Manufactured Hierarchical Stainless Steels with High Strength and Ductility. *Nat. Mater* 17, 63–71. doi:10.1038/nmat5021

Withers, P. J., Preuss, M., Steuwer, A., and Pang, J. W. L. (2007). Methods for Obtaining the Strain-free Lattice Parameter when Using Diffraction to Determine Residual Stress. *J. Appl. Cryst.* 40, 891–904. doi:10.1107/s0021889807030269

Wu, W., Chuang, C.-P., Qiao, D., Ren, Y., and An, K. (2016). Investigation of Deformation Twinning under Complex Stress States in a Rolled Magnesium alloy. *J. Alloys Comp.* 683, 619–633. doi:10.1016/j.jallcom.2016.05.144

Xu, C., Song, W., Pan, Q., Li, H., and Liu, S. (2015). Nondestructive Testing Residual Stress Using Ultrasonic Critical Refracted Longitudinal Wave. *Phys. Proced.* 70, 594–598. doi:10.1016/j.phpro.2015.08.030

Conflict of Interest: The authors declare that the research was conducted in the absence of any commercial or financial relationships that could be construed as a potential conflict of interest.

Publisher's Note: All claims expressed in this article are solely those of the authors and do not necessarily represent those of their affiliated organizations, or those of the publisher, the editors, and the reviewers. Any product that may be evaluated in this article, or claim that may be made by its manufacturer, is not guaranteed or endorsed by the publisher.